Journal of Physics: Conference Series **655** (2015) 012024 doi:10.1088/1742-6596/655/1/012024

Thermal design of spacecraft solar arrays using a polyimide foam

N Bianco[1], M Iasiello[1,2] and V Naso[1]

[1] Dipartimento di Ingegneria Industriale (DII) – Università degli studi di Napoli Federico II – P.le Tecchio, 80 – 80125 – Napoli -Italy,

Abstract. The design of the Thermal Control System (TCS) of spacecraft solar arrays plays a fundamental role. Indeed, the spacecraft components must operate within a certain range of temperature. If this doesn't occur, their performance is reduced and they may even break. Solar arrays, which are employed to recharge batteries, are directly exposed to the solar heat flux, and they need to be insulated from the earth's surface irradiation. Insulation is currently provided either with a white paint coating or with a Multi Layer Insulation (MLI) system [1]. A configuration based on an open-cell polyimide foam has also been recently proposed [2]. Using polyimide foams in TCSs looks very attractive in terms of costs, weight and assembling. An innovative thermal analysis of the above cited TCS configurations is carried out in this paper, by solving the porous media energy equation, under the assumption of Local Thermal Equilibrium (LTE) between the two phases. Radiation effects through the solar array are also considered by using the Rosseland approximation. Under a stationary daylight condition, temperature profiles are obtained by means of the finite-element based code COMSOL Multiphysics®. Finally, since the weight plays an important role in aerospace applications, weights of the three TCS configurations are compared.

Nomenclature

$\boldsymbol{G}$	Incident heat flux (W/m^2)
i	Current layer
H	Length of the computational domain (m)
k	Thermal conductivity (W/m·K)
L	Length (m)
n	Effective index of refraction
N	Layers number
$\boldsymbol{q}$	Heat flux (W/m^2)
$\boldsymbol{s}$	MLI thickness (m)
T	Temperature (K)
x, y	Rectangular coordinates (m)
V	Volume (m^3)

Greek letters

α	Absorptivity
β	Extinction coefficient (1/m)
ε	Emittance
ρ	Density (kg/m^3)
σ	Stefan-Boltzmann constant (W/m^2 K^4)

Subscripts

al	aluminum
c	conduction
eff	effective
i	layer
MLI	Multi Layer Insulation
p	polyimide
r	radiation
s	solar
sc	cover glass
wp	white paint

Other symbols

$< >$	Volume average of a variable
∇	Nabla operator

[2] To whom any correspondence should be addressed. E-mail: marcello.iasiello@unina.it

1. Introduction

Thermal management of a space solar array is a primary task during its design phases. An example of the importance of this task is that internal electronic components of the spacecraft need to operate in certain temperature ranges. Solar arrays are employed to catch energy from the sun and convert into electricity. The solar cell efficiency, the ratio of the output electrical power to the incident radiation, is inversely proportional to its temperature; then, a correct thermal management guarantees the cells to operate into acceptable efficiency ranges [3].

The thermal heat rates involved on a satellite is sketched in figure 1. The absorbed fraction of the solar irradiation enters the satellite across its boundary facing the sun while the absorbed fraction of the sum of the earth albedo and the heat rate emitted by the earth enters the satellite across its boundary facing the earth. Heat rates emitted by both boundaries exit the satellite. Other heat rates can be neglected [2]. The control of the cell temperature requires to reduce the heat rate entering the boundary facing the earth. This is currently attained either coating it with a white paints [1] or affixing a multi layer insulation (MLI) system on it. The white paint coating AZW-LA-II has the best performances in terms of high emittance and low absorptance [4]. However, this solution has a high impact on costs of the insulation system [5]. Less expensive white paints are also employed. It is worth noticing that degradation of the coating optical properties can occur after many hours of operation [6]. On the other side, multilayer insulations allow to increase the thermal resistance, thus lowering the temperature of the solar cell. However, difficulties in assembling multilayer insulations are a drawback [2].

The above mentioned limitations can be overcome by using a polyimide foam insulation material on the rear of the solar array [2]. A high temperature polyimide foam for space applications, named LaRC TEEK, is manufactured by NASA Langley Research Center [7]. It has excellent flammability resistance, thermal insulation, cryogenic capability and a low weight. Compared to traditional systems, performances in terms of costs, easiness of assembly and weight can be also improved. In the present paper, a solar array configuration with a polyimide foam is proposed, and its thermal analysis is carried out. Results are compared with the thermal analysis of traditional Thermal Control Systems (TCS) of solar arrays.

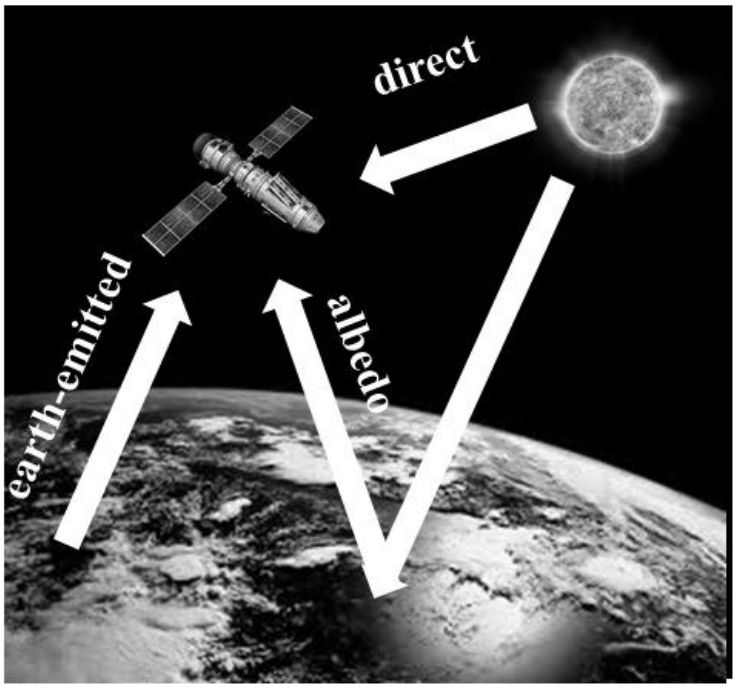

Figure 1. Thermal heat rates on a satellite.

2. Solar array design

The configurations of traditional space solar arrays are sketched in figures 2(a) [8] and 2(b) [1], for the white paint and MLI configurations, respectively. In both cases, solar cells are covered with a thin protective glass. Carbon-Fiber Reinforced Plastic (CFRP) is used to link the cell with the rest of the array. A honeycomb substrate is used for mechanical purposes and because of the high thermal resistance provided by its porosity. The bottom of the array can be coated with a white paint. In the multi-layer configuration (figure 2(b)), Kapton external sheets and aluminized Kapton internal sheets are employed. Sheets are separated by spacers, and the heat conduction between the sheets can be neglected. It is worth remarking that the MLI configuration is thicker than the white painted one. The configuration proposed by Zaglauer and Pitz [9], with an insulating open cell polyimide foam inserted between the honeycomb and the solar cell, is sketched in figure 2(c). The above mentioned configurations will be referred to in this paper.

3. Mathematical model

3.1. Governing equations

The thermal analysis of the TCS of solar arrays reported in figure 2 is carried out by solving the energy equation in steady-state condition.

For non-porous layers one can write:

$$\nabla^2 T = 0 \tag{1}$$

where T is the temperature.

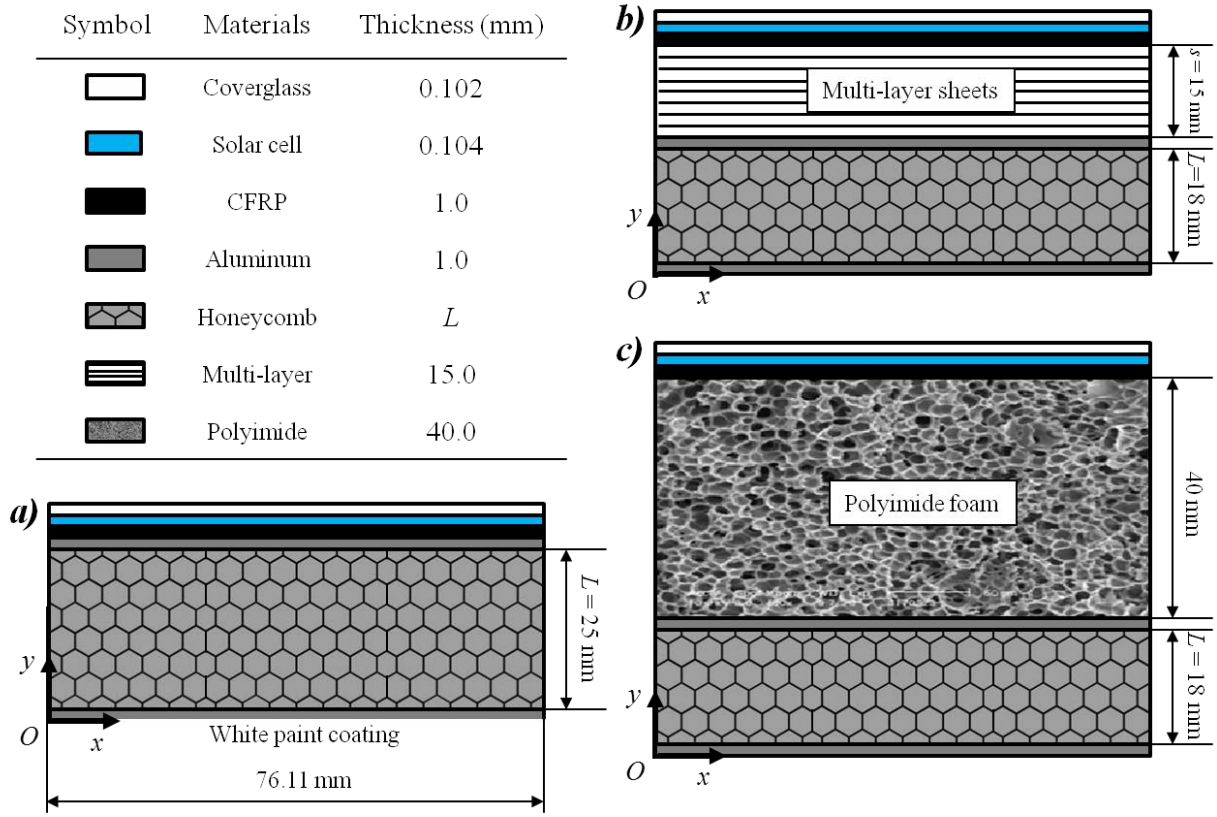

Figure 2. Space array configurations: a) with white paint; b) with MLI system; c) with polyimide foam.

For the open cell polyimide foam and the honeycomb layers, because of their porous nature, the energy equation is volume-averaged over a Representative Elementary Volume (REV) of the foam [10] and then solved for the whole porous domain. The averaged temperature is:

$$\langle T \rangle = \frac{1}{V} \int_V T \, dV \tag{2}$$

where V is the REV volume. The volume-averaged energy equation, under Local Thermal Equilibrium (LTE) between the two phases [11], is:

$$k_c \nabla^2 \langle T \rangle - \nabla \cdot \boldsymbol{q}_r = 0 \tag{3}$$

where k_c is the effective thermal conductivity of the porous material and $\boldsymbol{q}_r$ is the radiative heat flux. The radiative heat flux in porous media is usually described by solving the Radiative Transfer Equation (RTE) [12]. However, when the medium is optically thick, Rosseland approximation for radiation can be employed [13]. The radiative heat flux $\boldsymbol{q}_r$ can be calculated by means of the Fourier law:

$$\boldsymbol{q}_r = -k_r \nabla T \tag{4}$$

where the radiative thermal conductivity k_r is defined as [13]:

$$k_r = -\frac{16 \sigma n^2 T^3}{3 \beta(T)} \tag{5}$$

with σ the Stefan-Boltzmann constant, n the effective index of refraction, equal to 1 since porosity of foams is usually high [13], and $\beta(T)$ the mean extinction coefficient in whole wavelength range.

Equations (4) and (5) can be combined as:

$$\boldsymbol{q} = \boldsymbol{q}_c + \boldsymbol{q}_r = -(k_c + k_r) \nabla T \tag{6}$$

where $\boldsymbol{q}$ is the total heat flux, due to conduction and radiation, and $\boldsymbol{q}_c$ is the conduction heat flux. Combining equations (4) and (6), equation (3) for porous layers becomes a temperature volume-averaged Laplace equation:

$$\nabla^2 \langle T \rangle = 0 \tag{7}$$

Governing equations (1) and (7) are solved with reference to the rectangular system of coordinate *Oxy*, depicted in figure 2.

3.2. Boundary conditions

Boundary conditions for equations (1) and (7) are presented in the following. All the domains are considered to be grey for the radiation. Side walls of the computational domains reported in figure 2 are assumed to be adiabatic.

On the top of the computational domain, namely the cover glass of the solar cell, the following net heat flux $|\boldsymbol{q}_s|$ boundary condition holds:

$$\left|\boldsymbol{q}_s\right| = \alpha_{sc}\left|\boldsymbol{G}_s\right| - \varepsilon_{sc}\sigma T_{sc}^4 \tag{8}$$

with $|\boldsymbol{G}_s|$ the solar incident heat flux, equal to 1,367 W/m^2, α_{sc} the effective absorptivity of the solar cell, ε_{sc} the emittance of the outer cover glass surface, T_{sc} its temperature. Reference will be made to α_s = 0.696 [8] and ε_{sc} = 0.899 [8] in the following.

On the bottom of the computational domain, namely the satellite cover facing the earth, the boundary condition is:

$$\left|\boldsymbol{q}_{bs}\right| = \alpha_{bs}\left|\boldsymbol{G}_{bs}\right| - \varepsilon_{bs}\sigma T_{bs}^4 \tag{9}$$

where $|\boldsymbol{G}_{bs}|$ is the radiative heat flux incident on the satellite bottom surface, because of the earth albedo and the infrared emission by the earth, equal to 650 W/m^2. For the MLI configuration in figure 2(b) and for the polyimide foam configuration in figure 2(c) reference will be made to $\alpha_{bs} \equiv \alpha_{al}$ = 0.15 [15] and $\varepsilon_{bs} \equiv \varepsilon_{al}$ = 0.030 [15]; for the white paint configuration in figure 2(b), $\alpha_{bs} \equiv \alpha_{wp}$ = 0.39 [8] and $\varepsilon_{bs} \equiv \varepsilon_{wp}$ = 0.88 [8] are assumed.

At the interface of each layer, the continuity of temperature and heat flux between two adjacent layers *i* and *i+1* holds:

$$T_i\big|_{y_-} = T_{i+1}\big|_{y_+} \tag{10}$$

$$-\left[\left(k_c + k_r\right)\right]_i \left.\frac{\partial T}{\partial y}\right|_{y_-} = -\left[\left(k_c + k_r\right)\right]_{i+1} \left.\frac{\partial T}{\partial y}\right|_{y_+} \tag{11}$$

3.3. Thermophysical properties

As far as non-porous materials are concerned, the following values of conduction conductivity, k_c, are assumed: 1.0 W/m K for the coverglass, 100.0 W/m K for the solar cell, 54.4 W/m K for the CFRP, 235.0 W/m K for the aluminum.

As far as porous materials are concerned, reference will be made to a total conductivity, made up by the sum of the conduction conductivity, k_c, and the radiation conductivity, k_r.

As to the multilayer sheets, a 0.12 W/m K [15] effective conduction conductivity of an N = 10 layers material, is assumed. Accounting for the rather low maximum difference in the temperatures of the cover glass and the bottom surface of the solar array, the effective radiation conductivity of the MLI can be expressed by:

$$k_r = 4\sigma T^3 \frac{s}{N\left(\dfrac{2}{\varepsilon_{MLI}} - 1\right) + 1} \tag{12}$$

with s the MLI thickness and ε_{MLI} = 0.14 [15].

The effective total conductivity of the honeycomb structure is assumed equal to 116.0 W/m K [1].

The effective total conductivity of the polyimide foam is made up by the sum of the conduction contribution, 0.001 W/m K [14] for a 0.965 porosity polyimide foam, and the radiation contribution, given by equation (5) with the mean extinction coefficient given by [14]:

$$\beta\left(T\right) = \rho_p\left(17.4 + 0.229T - 2.27\cdot 10^{-4}T^2\right) \tag{13}$$

where ρ_p is the polyimide foam relative density.

3.4. Numerical solution

Governing equations (1) and (7), with boundary conditions described in the previous subsections, were solved by using the finite-element commercial code COMSOL Multiphysics. A triangular mesh was used for the discretization of the domain, with less than 25,000 elements in each simulated case. Grid

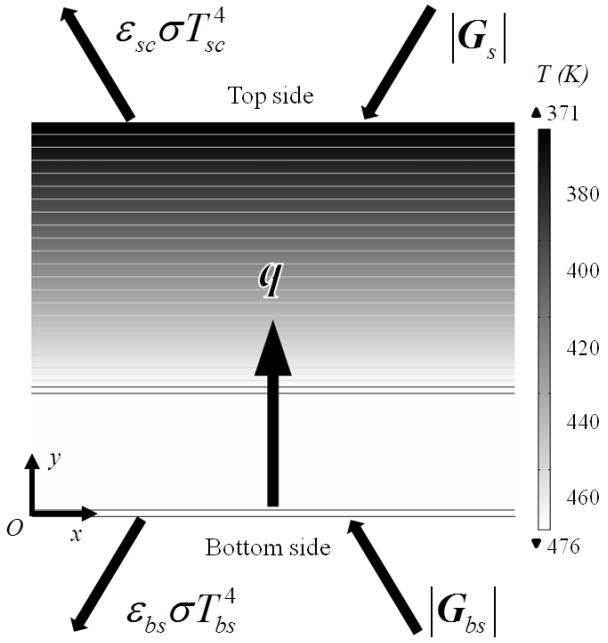

Figure 3. Temperature field in the TCS with polyimide foam.

independence was checked by performing simulations with 50,000 and 100,000 elements, that showed negligible differences in solar cell temperature fields. A convergence criterion of 10^{-4} was used, while the accuracy of energy balances was verified with a 10^{-10} order error.

4. Results

The temperature field in the TCS with the polyimide foam is shown in figure 3. The maximum temperature (about 470 °C) is attained on the back cover of the array. The temperature of the solar cell is about 370 K.

Temperature profiles in the TCSs of solar arrays in figure 2 are reported in figures 4 – 6. They show that the temperature of the solar cell is about 330 K for the white paint configuration and nearly 370 K for the MLI and the polyimide foam configurations. We can also notice that temperature gradients in the MLI and in the polyimide foam are negligible. Temperature is uniform in the honeycomb, because of its higher thermal conductivity than that of other materials.

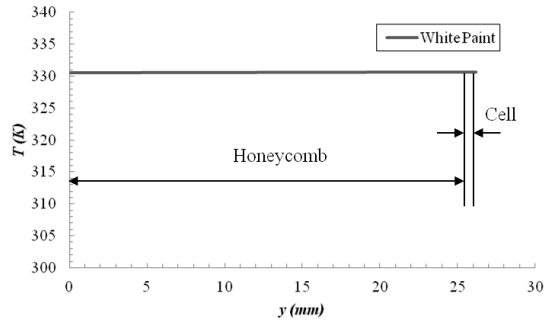

Figure 4. Temperature profile in the white paint configuration.

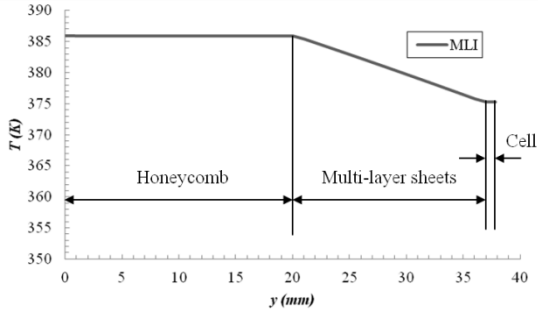

Figure 5. Temperature profile in the MLI configuration.

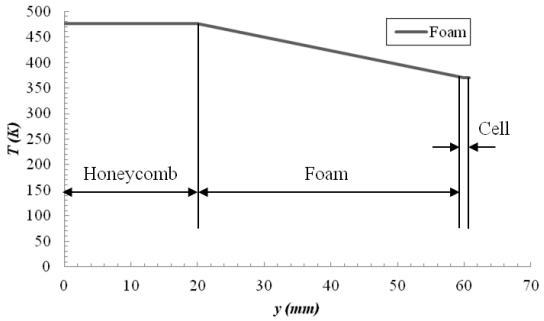

Figure 6. Temperature profile in the polyimide foam configuration.

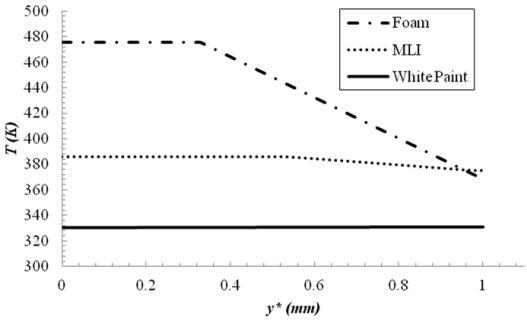

Figure 7. Comparisons of temperature profiles in different configurations.

For the sake of comparison, temperature profiles as a function of the dimensionless coordinate $y^* = y/H$, with H the length of the computational domain, that is the distance between the outer surfaces of the cover glass and the bottom cover of the satellite, are presented in figure 7. Even if the white paint configuration provides the lowest value of the cell temperature, it is worth reminding that the white paint has a high influence on the TCS overall costs. Besides, it is the configuration for which the weight becomes higher than the other two configurations, and the weight has a primary role in aerospace applications.

The weight of the three configurations is reported in table 1. Because, of structural reasons, the honeycomb of the latter device is thicker (25 mm) than in other two cases (18 mm). Therefore, one can notice that the polyimide foam configuration has the lowest weight, and the white paint configuration has the highest one. This implies that the polyimide foam has an advantage in terms of weight.

Table 1. Weights of space solar arrays.

Configuration	Weight (kg)
White paint	0.202
MLI	0.177
Polyimide foam	0.166

5. Conclusions

An innovative thermal analysis of some Thermal Control System (TCS) of spacecraft solar arrays has been presented. Temperature profiles have been compared by using a finite-element method. Results showed that the temperature reached on a polyimide foam based TCS is low enough to allow a proper operation of the solar cell. A comparison between the three configurations in terms of weight showed that the polyimide foam can be used to insulate a space solar array by reducing the weight of the solar array, in addition to the other mentioned advantages of costs, assembling and longevity.

6. References

[1] Gilmore D G *et al.* 2002 Thermal design examples *Spacecraft Thermal Control Handbook vol. 1 Fundamental Technologies* ed D G Gilmore (El Segundo, CA: The Aerospace Press) chapter 3 pp 71 - 137

[2] Wolters R 2001 Structure of thermal insulation of satellites US6318673 (Patent)

[3] Skoplaki E and Palyvos J A 2009 On the temperature dependence of photovoltaic module electrical performance: A review of efficiency/power correlations *Sol. Energy* **83** 614-24

[4] Choi M K 2004 AZW-LA-II White paint on swift: lessons learned from first time flying on spacecraft radiators *Proc. 2nd International Energy Conversion Engineering Conference (Providence, RI, 16 – 19 August 2004)*
[5] Anvari A, Farhani F and Niaki K S 2009 Comparative study on space qualified paints used for thermal control of a small satellite *IJChE* **6** 50-62
[6] Ding Y, Feng W and Yan D 2009 Degradation of optical-properties of thermal control coatings under space low energy electrons Proc. 11th International Symposium On Materials in a Space Envionment (Aix-en-Provence, France, 15 – 18 September 2009)
[7] Pater R H and Curto P A 2007 Advanced materials for space applications *Acta Astronaut.***61** 1121-9
[8] Kim H K and Han C Y 2010 Analytical and numerical approaches of a solar array thermal analysis in a low-earth orbit satellite *Adv. Space Res.* **46** 1427-39
[9] Zaglauer A and Pitz W 2003 Champ-The first flexbus in orbit *Acta Astronaut.* **52** 747-51
[10] Nakayama A and Kuwahara F 2008 A general bioheat transfer model based on the theory of porous media *Int. J. Heat Mass Tran.* **51** 3190-99
[11] Amiri A and Vafai K 1994 Analysis of dispersion effects and non-thermal equilibrium, non-Darcian, variable porosity incompressible flow through porous media *Int. J. Heat Mass Tran.* **37** 939-54
[12] Coquard R, Rochais D and Baillis D 2010 Conductive and radiative heat transfer in ceramic and metal foams at fire temperatures *Fire Technol.* **48** 699-732
[13] Baillis D and Coquard R 2008 Radiative and conductive thermal properties of foams *Cellular and Porous Materials: Thermal Properties Simulation and Prediction* ed A. Öchsner, G E Murch and M. J. S. de Lemos (Weinheim: Wiley-VCH) chapter 11 pp 343-384
[14] Caps R, Heinemann U, Fricke J and Keller K 1997 *Int. J. Heat Mass Tran.* **40** 269-80
[15] Donabedian M, Gilmore D G, Stultz J W, Tsuyuki G T and Lin E I 2002 Thermal design examples *Spacecraft Thermal Control Handbook vol. 1 Fundamental Technologies* ed D G Gilmore (El Segundo, CA: The Aerospace Press) chapter 5 pp 161-205